2′,7′-Difluorofluorescein Excited-State Proton Reactions: Correlation between Time-Resolved Emission and Steady-State Fluorescence Intensity

Angel Orte,[†] Ruperto Bermejo,[‡] Eva M. Talavera,[†] Luis Crovetto,[†] and Jose M. Alvarez-Pez*[,†]

Department of Physical Chemistry, University of Granada, Cartuja Campus, 18071 Granada, Spain, and Department of Physical and Analytical Chemistry, University of Jaén, E.U.P. of Linares, 23700 Linares, Spain

Received: November 22, 2004; In Final Form: January 19, 2005

The presence of excited-state buffer-mediated proton exchange reactions influences the steady-state fluorescence signals from dyes in solution. Since biomolecules in general have some chemical groups that can act as proton acceptors/donors and are usually dissolved in buffer solutions which can also behave as appropriate proton acceptors/donors, the excited-state proton exchange reactions may result in distorted steady-state fluorescence signals. In a previous paper (*J. Phys. Chem. A* **2005**, *109*, 734−747), we evaluated kinetic and other pertinent parameters for the excited-state proton reactions of the prototropic forms of 2′,7′-difluorofluorescein (Oregon Green 488, OG488), recording a fluorescence decay surface at different pH values and acetate buffer concentrations, analyzed by means of global compartmental analysis. In this article we use the rate constants and the corrected pre-exponential factors from the previously recorded fluorescence decay traces to simulate the decay times and associated pre-exponentials at different acetate buffer concentrations and constant pH and compare these theoretically calculated values with new experimental data. We also calculate the steady-state fluorescence intensity vs pH and vs acetate buffer concentration (at constant pH) and compare these calculated emission values with the experimental data previously published. The agreement between the experimental and simulated data is excellent.

Introduction

2′,7′-Difluorofluorescein (Oregon Green 488, OG488) is a new fluorescein-based dye,[1] whose use has become very popular in recent years as a fluorescent probe in biomedicine, biochemistry, neurosciences, etc.[1,2] Depending on pH, the dye can exist in solution as cation, neutral, monoanion, or dianion. The cation form is present only at low pH, and only neutral, monoanion, and dianion forms are significant in the pH range 3.30−9.00.

For several years, we have been investigating the excited-state proton exchange reactions of fluorescein and the effect of suitable proton acceptors/donors which promote these reactions.[3,4] The presence of these excited-state reactions may appreciably influence the steady-state fluorescence signals when using these dyes. The description of the reactions is thus a matter of great interest.

In a previous paper,[5] we showed by steady-state and time-resolved fluorescence measurements that excited OG488 molecules can undergo neutral−monoanion excited-state proton transfer reaction, whereas excited monoanion and dianion interconvert each other only if a suitable proton acceptor/donor, such as the species of acetate buffer, is present in solution. We found that the latter reaction becomes experimentally noticeable at acetate buffer concentrations above 10 mM and increases in efficiency as the buffer concentration is increased. We recovered the rate constant values for deactivation of the monoanion (2.94×10^8 s^{-1}) and dianion (2.47×10^8 s^{-1}), as well as the rate constant values of the buffer-mediated excited-state deprotonation and protonation (9.70×10^8 M^{-1} s^{-1} and 1.79×10^8 M^{-1} s^{-1}, respectively). The kinetics of the reaction was solved by using the global compartmental analysis approach[6] under identifiability conditions.[7] With the recovered rate constant values, an apparent $pK_a^* = 4.02$ was obtained.

As indicated previously, when these kind of excited-state proton transfer reactions take place, they influence the steady-state fluorescence signals and could cause misinterpretion of the experimental data from the dye. Since proteins and biomolecules in general have chemical groups that can act as proton acceptors/donors and the buffer in which they are dissolved can also behave as an appropriate proton acceptor/donor, the excited-state reactions may result in distorted steady-state fluorescence signals when the dye is used for labeling biomolecules, as a pH or Ca^{2+} probe, etc. Nevertheless, the specific rate constants, which we evaluated in the previous paper, are very good at predicting time-resolved and steady-state emission data and can thus contribute to a better interpretation of the experimental steady-state fluorescence intensity from the probe.

In this article, we examine how well the specific rate constants, along with the time-resolved emission data, correlate with steady-state fluorescence spectra. More specifically, we use the time-resolved emission data to calculate the steady-state fluorescence intensity vs pH at 1 M acetate buffer concentration and compare the results with the corresponding fluorescence signals at different pH values. Moreover, we predict the decay times for aqueous solutions of OG488 at a constant pH and different acetate buffer concentrations and compare these with experimental data. Finally, we simulate the previously published steady-state fluorescence signals vs acetate concentration at constant pH values.

Theoretical Relationships between Time-Resolved Emission and Steady-State Fluorescence Intensity

Scheme 1 represents the dynamic, linear, time-invariant, intermolecular system used in the previous paper to describe the considered dye.[5] It consists of two distinct types of ground-state species and their corresponding excited-state species. **1** and **2** are different prototropic forms of the dye. Thus, the

* To whom correspondence should be addressed. E-mail: jalvarez@ugr.es.
[†] University of Granada.
[‡] University of Jaén.

10.1021/jp044681m CCC: $30.25 © 2005 American Chemical Society
Published on Web 03/08/2005

SCHEME 1: Kinetic Model of an Excited-State Buffer-Mediated Proton Transfer Reaction[a]

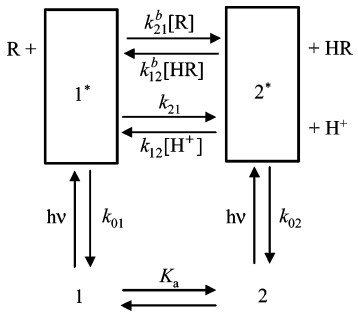

[a] **1** and **2** are the ground-state conjugate acid−base forms of the fluorophore, whereas **1*** and **2*** are the corresponding excited species. R and HR are the acid−base species of the proton acceptor/donor.

ground-state species are related through the acid−base equilibria, determined by the corresponding pK_a. Excited-state species **1*** and **2*** are created upon photoexcitation and can decay by fluorescence (F) and nonradiative (NR) processes. These decay processes are included in the rate constant k_{0i} ($=k_{Fi} + k_{NRi}$) for species *i**. In this study we consider the excited-state process promoted by species of a suitable proton acceptor/donor: the species of a buffer, HR and R. The concentrations of HR and R are related to the pH through the equilibrium constant pK_a^{buff} and the total buffer concentration C^{buff}. The protonation of **2*** mediated by HR is represented by rate constant k_{12}^b. Likewise, R could act as a proton acceptor resulting in an excited-state deprotonation of **1***, whose rate constant is denoted by k_{21}^b. We also include the deprotonation of excited state **1*** (represented by rate constant k_{21}) and excited-state reaction of **2*** with aqueous protons, with the rate constant denoted by k_{12}.

If the system represented by Scheme 1 is excited with a δ-pulse, which does not significantly alter the concentrations of the ground-state species, the time course of the excited species is given by the following differential equation:

$$\dot{\mathbf{x}}(t) = \mathbf{A}\mathbf{x}(t) \tag{1}$$

where **A** is the matrix describing the processes which occur during the excited species lifetime, given by[5]

$$\mathbf{A} = \begin{bmatrix} -(k_{01} + k_{21} + k_{21}^b[\mathrm{R}]) & k_{12}[\mathrm{H^+}] + k_{12}^b[\mathrm{HR}] \\ k_{21} + k_{21}^b[\mathrm{R}] & -(k_{02} + k_{12}[\mathrm{H^+}] + k_{12}^b[\mathrm{HR}]) \end{bmatrix} \tag{2}$$

The vector $\dot{\mathbf{x}}(t)$ denotes the time first-order derivative of $\mathbf{x}(t)$, vector of the concentrations of species **1*** and **2***. The solutions of the coupled differential rate equations given the time course of excited species are the well-known biexponential expressions:[8]

$$x(t) = \begin{pmatrix} [\mathbf{1}^*](t) \\ [\mathbf{2}^*](t) \end{pmatrix} = \begin{pmatrix} \beta_{11}e^{\gamma_1 t} + \beta_{12}e^{\gamma_2 t} \\ \beta_{21}e^{\gamma_1 t} + \beta_{22}e^{\gamma_2 t} \end{pmatrix} \tag{3}$$

where γ_i are the eigenvalues of the matrix **A** and are given by

$$\gamma_{1,2} = \frac{a_{11} + a_{22} \pm \sqrt{(a_{22} - a_{11})^2 + 4a_{12}a_{21}}}{2} \tag{4}$$

with a_{ij} being the *ij*th element of the matrix (eq 2).

The γ_i factors are related to the decay times τ_i by the expression

$$\tau_i = -\frac{1}{\gamma_i} \tag{5}$$

The overlap between the absorption spectra of the species **1** and **2** results in the direct excitation of both at time zero by the δ-pulse of light. Using the initial concentrations $[\mathbf{1}^*]_0$ and $[\mathbf{2}^*]_0$ produced by the light pulse as initial conditions, the following expressions for the four pre-exponential factors of eq 3 are obtained:

$$\beta_{11} = \frac{[\mathbf{1}^*]_0(\gamma_2 - a_{11}) - a_{12}[\mathbf{2}^*]_0}{\gamma_2 - \gamma_1} \tag{6a}$$

$$\beta_{12} = -\frac{[\mathbf{1}^*]_0(\gamma_1 - a_{11}) - a_{12}[\mathbf{2}^*]_0}{\gamma_2 - \gamma_1} \tag{6b}$$

$$\beta_{21} = \frac{[\mathbf{2}^*]_0(\gamma_2 - a_{22}) - a_{21}[\mathbf{1}^*]_0}{\gamma_2 - \gamma_1} \tag{6c}$$

$$\beta_{22} = -\frac{[\mathbf{2}^*]_0(\gamma_1 - a_{22}) - a_{21}[\mathbf{1}^*]_0}{\gamma_2 - \gamma_1} \tag{6d}$$

The decay of fluorescence intensity following excitation by the δ-pulse of light is given by the expression

$$f(\lambda^{ex},\lambda^{em},t,C^{buff},\mathrm{pH}) = \kappa(c_1[\mathbf{1}^*] + c_2[\mathbf{2}^*]) = p_1e^{\gamma_1 t} + p_2e^{\gamma_2 t} \quad t \geq 0 \tag{7}$$

where κ is an instrumental factor, depending on λ^{ex} and λ^{em}, and c_i are the emission weighting factors of species *i** at the experimental λ^{em}, defined by[9]

$$c_i(\lambda^{em}) = k_{Fi}\int_{\Delta\lambda^{em}} \rho_i(\lambda^{em})\, d\lambda^{em} \tag{8}$$

In eq 8 k_{Fi} is the fluorescence rate constant of *i**; $\Delta\lambda^{em}$ is the emission wavelength interval around λ^{em} where the fluorescence signal is monitored; $\rho_i(\lambda^{em})$ is the emission density of *i** at λ^{em}, defined by[9]

$$\rho_i(\lambda^{em}) = F_i(\lambda^{em},\lambda^{ex}) / \int_{\text{full emission band}} F_i(\lambda^{em},\lambda^{ex})\, d\lambda^{em} \tag{9}$$

where the integration extends over the whole steady-state fluorescence spectrum F_i of species *i**.

Thus, the pre-exponential factors p_i are given by

$$p_1 = \kappa(c_1\beta_{11} + c_2\beta_{21}) \tag{10a}$$

$$p_2 = \kappa(c_1\beta_{12} + c_2\beta_{22}) \tag{10b}$$

Substituting β_{ij} into eqs 10, we obtain the following expressions for the pre-exponential factors:

$$p_1 = \kappa \times \frac{c_1[[\mathbf{1}^*]_0(\gamma_2 - a_{11}) - a_{12}[\mathbf{2}^*]_0] + c_2[[\mathbf{2}^*]_0(\gamma_2 - a_{22}) - a_{21}[\mathbf{1}^*]_0]}{\gamma_2 - \gamma_1} \tag{11a}$$

$$p_2 = -\kappa \times \frac{c_1[[\mathbf{1}^*]_0(\gamma_1 - a_{11}) - a_{12}[\mathbf{2}^*]_0] + c_2[[\mathbf{2}^*]_0(\gamma_1 - a_{22}) - a_{21}[\mathbf{1}^*]_0]}{\gamma_2 - \gamma_1} \tag{11b}$$

$[\mathbf{1}^*]_0$ and $[\mathbf{2}^*]_0$ are functions of ground-state concentrations of **1** and **2** and the molar extinction coefficients ϵ_1 and ϵ_2 at the

excitation wavelength. In turn, the ground-state concentrations are functions of pH and the dissociation constant K_a for the reversible reaction $\mathbf{1} \leftrightarrows \mathbf{2} + H^+$. Thus, the relationships between kinetic rate constants (and related parameters) and the weighting coefficients are given by

$$p_1 = \frac{\kappa C_t}{\gamma_2 - \gamma_1} \frac{c_2[\epsilon_2^{\lambda^{ex}} K_a(\gamma_2 - a_{22}) - \epsilon_1^{\lambda^{ex}} a_{21}[H^+]] + c_1[\epsilon_1^{\lambda^{ex}}[H^+](\gamma_2 - a_{11}) - a_{12}K_a\epsilon_2^{\lambda^{ex}}]}{K_a + [H^+]} \quad (12a)$$

$$p_2 = -\frac{\kappa C_t}{\gamma_2 - \gamma_1} \frac{c_2[\epsilon_2^{\lambda^{ex}} K_a(\gamma_1 - a_{22}) - \epsilon_1^{\lambda^{ex}} a_{21}[H^+]] + c_1[\epsilon_1^{\lambda^{ex}}[H^+](\gamma_1 - a_{11}) - a_{12}K_a\epsilon_2^{\lambda^{ex}}]}{K_a + [H^+]} \quad (12b)$$

where $\epsilon_i^{\lambda^{ex}}$ represents the molar extinction coefficient of species i at λ^{ex}, and C_t denotes the total concentration of the dye.

When the system is excited with light of constant intensity (at sample absorbance < 0.1), the steady-state fluorescence signal observed at λ^{em} upon excitation at λ^{ex} is given by

$$F(\lambda^{ex},\lambda^{em},C^{buff},\mathrm{pH}) = \chi\int_0^\infty f(\lambda^{ex},\lambda^{em},t,C^{buff},\mathrm{pH})\,dt = -\chi\left(\frac{p_1}{\gamma_1} + \frac{p_2}{\gamma_2}\right) \quad (13)$$

This equation states that the steady-state intensity is proportional to the area under the graph of $f(\lambda^{ex},\lambda^{em},t,C^{buff},\mathrm{pH})$ vs t, or the sum of all photons detected from $t = 0$ to ∞ after excitation by an instantaneous pulse of light. χ is an instrumental constant, depending on λ^{ex} and λ^{em}.

Fluorescence decay traces are usually collected with 10^4 counts in the peak channel, in different time intervals and under different optical conditions. Thus, these decay traces lack amplitude information and the values of the weighting coefficients obtained from these decay traces cannot be directly related to eqs 12. To obtain values of p_1 and p_2 that can be analyzed by eqs 12 at different pH values, it is necessary to evaluate them from fluorescence decay traces whose relative amplitudes have been adjusted so that they are equivalent to those recorded for the same time interval and the same optical setup. This correction of the pre-exponential factors will be detailed in the next section.

Materials and Methods

Reagents and Solutions. 2′,7′-Difluorofluorescein (Oregon Green 488) was purchased from Molecular Probes (Eugene, OR). Acetic acid (HOAc), sodium acetate (NaOAc), and sodium hydroxide were from Merck and were used without further purification. A stock solution of 2′,7′-difluorofluorescein (10^{-4} M) in 1.27×10^{-3} M NaOH was prepared using MilliQ water. Using this stock solution, different solutions 5×10^{-6} M in OG488 were prepared, at a neutral pH, with [NaOAc] = 1.5 M, and with [HOAc] = 1.5 M. We mixed the required volumes of these three solutions to reach a fixed pH value of 4.6 and the total buffer concentrations required. Solutions were kept cool in the dark when not in use to avoid possible deterioration by exposure to light and heat as occurs in fluorescein.[10] In this paper we use some experimental data previously published.[5] For reagents and solutions used in those experiments, the latter paper should be consulted.

Absorption and Steady-State Fluorescence Measurements. Absorption spectra were recorded on a GBC Cintra 10e UV−vis spectrophotometer with a temperature-controlled cell holder. A Perkin-Elmer LS 55 spectrofluorometer with a temperature-controlled cell holder was used to acquire steady-state fluorescence emission and excitation spectra. All measurements were made at room temperature, and 10×10 mm cuvettes were used for both absorption and steady-state fluorescence measurements.

Time-Resolved Fluorescence Measurements. Fluorescence decay traces were recorded on an Edinburgh Analytical Instrument FL900 ns time-resolved spectrofluorometer operating in the time-correlated single photon counting mode. This system employs a free running discharge flashlamp (nF900 Nanosecond Flashlamp) operating at 7.0 kV, 0.40 bar (H_2), and a frequency of 40 kHz, providing a lamp pulse of 0.8 ns (fwmh). Fluorescence decay traces were collected using 10×10 mm cuvettes, along 1024 channels of the multichannel analyzer with a time-per-channel of 48 ps. Histograms of the instrument response function (recorded using a light scattering solution, LUDOX Colloidal silica, Sigma), and sample decays were recorded until reaching the typical value of 10^4 counts at the maximum.

We recorded decay traces of OG488 solutions with increasing total buffer concentration (in a range between 0.1 and 1 M) at a fixed pH (4.60). The experimental setups used were as follows: $\lambda^{ex} = 420$ nm and $\lambda^{em} = 515$ nm; $\lambda^{ex} = 440$ nm and $\lambda^{em} = 515$ nm; $\lambda^{ex} = 440$ nm and $\lambda^{em} = 550$ nm. These conditions produce preferential excitation of the monoanion and preferential detection of the dianion emission.

The decay traces were globally analyzed by means of usual deconvolution methods, based on Marquardt's algorithm, using multiexponential functions as decay laws. The decay times were shared parameters, linked over decays at the same buffer concentration, whereas the pre-exponential factors were local adjustable parameters.

Evaluation of Corrected Pre-exponentials. All fluorescence decay traces for different pH values and 1 M acetate buffer concentration, analyzed through global and global compartmental analysis in our previous paper,[5] were recorded with 10^4 counts at the peak channel in the usual manner. Due to the different emission intensities of each sample and the modification of the optical settings of the instrument in each decay, the pre-exponential values recovered from these global analyses cannot be related directly to eqs 12. To fit the model to the recovered pre-exponentials, it is necessary to calculate the pre-exponentials equivalent to those recorded for the same time interval under the same optical conditions.

With the spectrofluorimeter operating in the single photon mode and with fixed instrument settings, we recorded the number of total counts for each sample during a fixed, short time interval (=5 min). The number of total counts recorded for the different samples is proportional to the relative areas $A(\mathrm{pH}_i)$ under the decay traces when recorded for the same time interval with identical instrument settings, and hence proportional to the steady-state fluorescence emission. That is, $A(\mathrm{pH}_i) = \int_0^\infty f_{5\mathrm{min}}(\lambda^{ex},\lambda^{em},t,\mathrm{pH})\,dt$. Let $NT(\mathrm{pH}_i) = \int_0^\infty f_{10000}(\lambda^{ex},\lambda^{em},t,\mathrm{pH})\,dt$ be the area under decay traces recorded with 10^4 counts at the peak channel (the number of total counts for the sample recorded during the time necessary to acquire 10^4 counts at the peak). The decay traces recorded with 10^4 counts at the peak channel were reduced to the graphs recorded for the same time interval by adjusting their areas so that their ratios were the same as $A(\mathrm{pH}_i)$. We calculate the adjustment factor $C(\mathrm{pH}_i)$ with the expression

$$C(\mathrm{pH}_i) = \frac{A(\mathrm{pH}_i)}{NT(\mathrm{pH}_i)}\sigma \tag{14}$$

where σ is an arbitrary factor which has the same value for all the decays and yields values of $C(\mathrm{pH}_i)$ which are in a range around 1. Finally, the pre-exponentials from decay traces with 10^4 counts at the peak were multiplied by $C(\mathrm{pH}_i)$, yielding the corrected relative pre-exponentials directly related to eqs 12.

Nonlinear Least-Squares Fitting. The fitting of the pre-exponential factors to the theoretical equations from the kinetic model was carried out by means of Origin 6.0 routines for global fitting based on Marquardt's algorithm. The goodness-of-fitting criteria were the regression coefficient (r^2), the visual similarity between the fitted function and the experimental data, and the dependency coefficient indicating whether the equation is overparametrized. A dependency value below 0.96 is acceptable.[11]

Results and Discussion

Correlation between Time-Resolved and Steady-State Fluorescence Intensity. For the experimental OG488−acetate buffer system, the general kinetic model shown in Scheme 1 was substituted by that in Scheme 2. Here **1** and **2** are represented, respectively, by the monoanion, M, and dianion, D, of OG488, M* and D* are the associated excited states of these species, and the proton acceptor/donor is the corresponding acetate buffer species. Thus, the model consists of only two distinct types of dye in the ground state and their corresponding excited-state species, as established in our previous paper where we demonstrated that neutral and monoanion species behave as a single compartment, due to their sufficiently rapid interconversion during the excited state and the same emissive behavior (quinoid configurations in the xanthene moiety) of both species. Thus, although three prototropic forms are present in the ground and excited states (neutral, monoanion, and dianion) in the considered pH range, the excited-state proton transfer (ESPT) process can be completely described by a two-state excited-state model.

In our previous paper, fluorescence decay traces of OG488 solutions, in the presence of 1 M acetate buffer, were recorded over a pH range between 3.30 and 9.12. The excitation wavelength was 420 nm, which produces preferential monoanion/neutral excitation. The emission wavelengths were 515, 525, 550, 570, and 600 nm. With these decay traces, standard global analyses (in terms of τ_i and p_i) were performed, linking decay times τ_i over all decay traces at the same pH, while pre-exponential factors p_i must be different at every emission wavelength and pH. The global analyses showed biexponential decay laws. The decay times were clearly pH-dependent, and the shorter decay time showed a negative pre-exponential. These

SCHEME 2: Kinetic Model of the Excited-State Proton Transfer Reaction between Monoanion (M) and Dianion (D) of OG488, Promoted by Acetic Acid/Acetate as Proton Acceptor/Donor

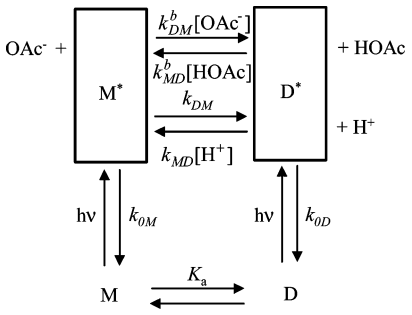

are characteristic features of an excited-state proton transfer promoted by a suitable proton acceptor/donor, resulting in a reversible excited-state reaction.

In the OG488 system, the short decay time is a rise-time at the emission wavelengths of 515, 525, 550, and 570 nm, since formation of D* from M* in the excited state leads to an increase in emission. But this does not happen at the 600 nm emission wavelength. At this λ^{em}, monoanion emission is higher than that of dianion, and the ESPT M* → D* produces a loss in emission at 600 nm. This results in a positive pre-exponential factor associiated with the shorter decay time at this emission wavelength.

To relate the time-resolved parameters, decay times, and pre-exponential factors with the steady-state fluorescence emission, the associated pre-exponential factors from global analyses of decay traces recorded with 10^4 counts at the peak channel must be corrected by multiplying them by the factors in eq 14, as described in Materials and Methods. We performed a global nonlinear least-squares fitting of the corrected pre-exponential factors from decays at the emission wavelengths 515, 525, 550, 570, and 600 nm, according to eqs 15, derived from eqs 12:

$$p_1 = \frac{\kappa'}{\gamma_2 - \gamma_1} \frac{[\epsilon_R^{\lambda^{ex}} K_a(\gamma_2 - a_{22}) - a_{21}[\mathrm{H}^+]] + c_R[[\mathrm{H}^+](\gamma_2 - a_{11}) - a_{12}K_a\epsilon_R^{\lambda^{ex}}]}{K_a + [\mathrm{H}^+]} \tag{15a}$$

$$p_2 = -\frac{\kappa'}{\gamma_2 - \gamma_1} \frac{[\epsilon_R^{\lambda^{ex}} K_a(\gamma_1 - a_{22}) - a_{21}[\mathrm{H}^+]] + c_R[[\mathrm{H}^+](\gamma_1 - a_{11}) - a_{12}K_a\epsilon_R^{\lambda^{ex}}]}{K_a + [\mathrm{H}^+]} \tag{15b}$$

where $\epsilon_R^{\lambda^{ex}}$ is the relative extinction coefficient ($\epsilon_2^{\lambda^{ex}}/\epsilon_1^{\lambda^{ex}}$), c_R is the relative emission weighting factor (c_1/c_2), and $\kappa' = \kappa C_t \epsilon_1^{\lambda^{ex}} c_2$ is a proportionality constant depending on λ^{ex} and λ^{em}. As derived from eqs 15, the corrected pre-exponential values permit the recovery of information on the molar extinction coefficients and the relative emission efficiencies of the species involved in the excited-state reaction, by fitting eqs 15 to these experimental data. In the global fitting process, the adjustable parameters were c_R, linked over pre-exponentials from decays recorded at the same λ^{em}, ϵ_R which was linked over all the pre-exponential factors (since a single λ^{ex} was used), and κ', linked over pre-exponentials associated with decays recorded at the same emission wavelength. The global fitting was carried out using the Origin NLLS fitting routines, based on Marquardt's algorithm. Figure 1 shows the corrected pre-exponential factors (symbols) and the fitting functions for each factor as lines. As can be seen, the fitting is very good, as is also demonstrated by the global regression coefficient, $r^2 = 0.997$, and dependency parameter values below 0.67. Table 1 shows the ϵ_R, c_R, and κ' values recovered. The ϵ_R value, 0.283, is slightly higher than that previously reported ($\epsilon_R^{420} = \epsilon_D^{420}/\epsilon_M^{420} = 0.221$)[5] by means of absorption measurements. Nevertheless, this slight difference may be a consequence of the different instruments and techniques used to obtain each ϵ_R. The recovered c_R values are also in good agreement with the results previously reported. We compared the recovered c_R with the ratio $\tilde{c}_M/\tilde{c}_D$ from ref 5, where $\tilde{c}_i$ is the emission parameter of species i recovered in the global compartmental analysis. As can be seen in Table 1, the agreement between the recovered c_R values and the reported $\tilde{c}_M/\tilde{c}_D$ is acceptable.

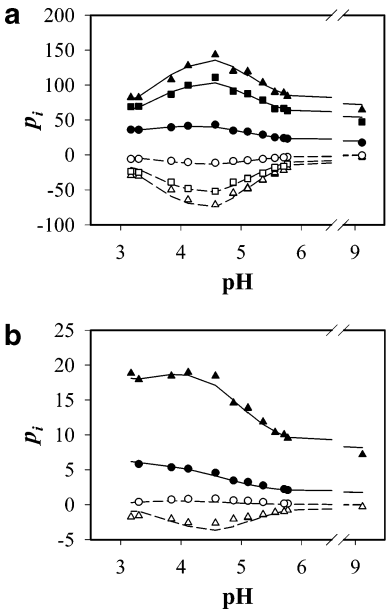

Figure 1. Corrected pre-exponential factors p_i recovered from global analyses (symbols) of decay traces from OG488 aqueous solutions at 1 M acetate buffer concentration, and global fitting functions (lines). Pre-exponentials associated with the longer decay time are represented by solid lines and filled symbols, while factors associated with the shorter decay time are plotted as dashed lines and blank symbols. (a) $\lambda^{ex} = 420$ nm and $\lambda^{em} = 515$ nm (▲ and △), 525 nm (■ and □), and 550 nm (● and ○). (b) $\lambda^{ex} = 420$ nm and $\lambda^{em} = 570$ nm (▲ and △), and 600 nm (● and ○).

TABLE 1: Recovered Parameters from the Global Fitting of Equations 15 to the Corrected Pre-exponential Factors vs pH

λ^{em} (nm)	ϵ_R^{420nm}	κ'	c_R	$\tilde{c}_M/\tilde{c}_D$[a]
515	0.283 ± 0.004	254 ± 2	0.210 ± 0.005	0.218
525		191 ± 2	0.248 ± 0.007	0.241
550		70 ± 2	0.45 ± 0.02	0.506
570		29 ± 2	0.60 ± 0.06	0.672
600		6.3 ± 0.2	1.05 ± 0.04	1.262

[a] From ref 5.

Using the recovered spectral parameters, the kinetic constants calculated in the previous paper,[5] and eqs 4, 13, and 15, we simulated the steady-state fluorescence signal expected at the excitation wavelength of 420 nm and emission wavelengths of 515, 525, 550, 570, and 600 nm, at the different pH values. We also recorded steady-state fluorescence intensity $F(\lambda^{ex},\lambda^{em},C^{buff},\text{pH})$ vs pH at 1 M acetate buffer concentration using two different experimental methods. The first method is based on eq 13 and works as follows: with the spectrofluorimeter in the single photon mode, we count all of the photons detected during 5 min. This number is the relative value of the integral $\int_0^\infty f_{5min}(\lambda^{ex},\lambda^{em},t,C^{buff},\text{pH})\,dt$, and we can equate it to relative steady-state fluorescence intensities of the samples, if the instrument settings are kept constant. The results of these measurements are shown as discrete solid points in Figure 2. For comparison, we have also included in the figure the previously published steady-state fluorescence intensity vs pH, measured by the conventional method using a standard steady-state spectrofluorimeter (blank symbols in Figure 2). Both values differ in amplitude because of different instrumental factors. We have therefore normalized the points so that they agree in amplitudes, within experimental errors. The solid curves drawn through the experimental points of Figure 2 were calculated with eqs 4, 13, and 15, using the parameters values shown in Table 1 and the recovered k_{ij} from our previous paper.[5] The

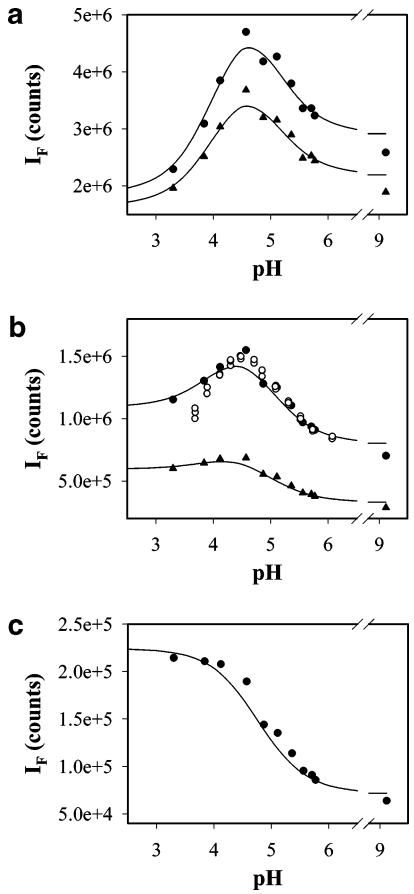

Figure 2. Total number of counts (filled symbols) acquired in 5 min under the same optical conditions of OG488 solutions in the presence of 1 M acetate buffer. The simulated steady-state intensities (lines) were calculated using the recovered parameters from Table 1, and $k_{0D} = 2.47 \times 10^8\ s^{-1}$, $k_{0M} = 2.94 \times 10^8\ s^{-1}$, $k_{MD} = 0$, $k_{DM} = 3.57 \times 10^6\ s^{-1}$, $k^b_{MD} = 1.79 \times 10^8\ M^{-1}\ s^{-1}$, and $k^b_{DM} = 9.70 \times 10^8\ M^{-1}\ s^{-1}$. (a) $\lambda^{ex} = 420$ nm and $\lambda^{em} = 515$ nm (●) and 525 nm (▲). (b) $\lambda^{ex} = 420$ nm and $\lambda^{em} = 550$ nm (●) and 570 nm (▲). Steady-state intensities recorded on a conventional fluorimeter, for $\lambda^{ex} = 420$ nm and $\lambda^{em} = 550$ nm, from ref 5, are also shown (○). (c) $\lambda^{ex} = 420$ nm and $\lambda^{em} = 600$ nm (●).

plots obtained directly from the theoretical calculation or simulation do not differ in amplitudes with respect to the experimental total number of counts, when multiplied by the factor used, σ, since instrumental factors are included in the recovered κ', as described above. It can be seen that the agreement between the experimental and simulated graphs is acceptable.

This approach, for recovering spectral information and correlating time-resolved and steady-state fluorescence signals, can also be performed through the ratio of the pre-exponential factors. In this case, the pre-exponential values do not need to be corrected. This could be useful if the total number of counts in a fixed time period is not acquired. In contrast, using the ratio yields a loss of half of the data to be fitted and a concomitant decrease in reliability.

From eqs 15, the following expression for the pre-exponentials ratio is obtained:

$$\frac{p_2}{p_1} = -\frac{[\epsilon_R^{\lambda^{ex}} K_a(\gamma_1 - a_{22}) - a_{21}[H^+]] + c_R[[H^+](\gamma_1 - a_{11}) - a_{12}K_a\epsilon_R^{\lambda^{ex}}]}{[\epsilon_R^{\lambda^{ex}} K_a(\gamma_2 - a_{22}) - a_{21}[H^+]] + c_R[[H^+](\gamma_2 - a_{11}) - a_{12}K_a\epsilon_R^{\lambda^{ex}}]} \quad (16)$$

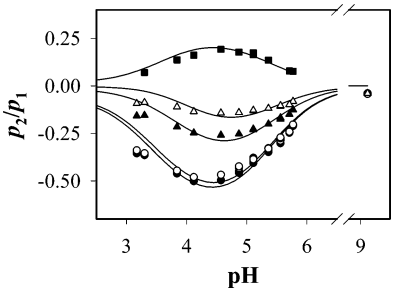

Figure 3. Ratio of the pre-exponential factors from Figure 1 (p_2/p_1, symbols) and global fitting functions (lines) from eq 16. $\lambda^{em} = 515$ (●), 525 (○), 550 (▲), 570 (△), and 600 nm (■).

TABLE 2: Recovered Parameters from the Global Fitting of Equation 16 to the Ratio of the Pre-exponential Factors vs pH

λ^{em} (nm)	ϵ_R^{420nm}	c_R
515	0.198 ± 0.008	0.29 ± 0.01
525		0.31 ± 0.01
550		0.55 ± 0.01
570		0.70 ± 0.01
600		1.20 ± 0.02

This equation can be globally fitted to the experimental ratios, in a similar procedure, to recover $\epsilon_R^{\lambda ex}$ and c_R. Figure 3 shows the fitting of eq 16 to the experimental data. The recovered values of the spectral parameters are collected in Table 2. The agreement is not as good as fitting the individual corrected pre-exponentials, as can be seen in Figure 3, and is derived from the r^2 value (0.982). The approach based on fitting the pre-exponentials ratio can be used to recover the spectral parameters rapidly; nevertheless, it shows some drawbacks: half of the experimental data are lost for performing the global fitting; in addition, the instrumental factors κ' are removed in eq 16, thus losing the relative information about different intensities at the different λ^{em} and requiring the simulated steady-state intensity to be normalized in order to be compared to the steady-state fluorescence emission.

Effect of the Total Acetate Buffer Concentration on the Fluorescence Emission. In this paper, we have also dealt with the influence of the total buffer concentration over the excited-state proton transfer reaction studied and the steady-state fluorescence signal. In our previous paper, the increase in steady-state fluorescence emission with increasing buffer concentration, at constant pH value, was demonstrated.[5] This increase is due to the deprotonation of the monoanion and the formation in the excited state of the dianionic form, which is much more fluorescent. In the present work, we extend this steady-state study, including time-resolved data of the influence of different total buffer concentrations on the excited-state reaction.

We have studied the absorption, steady-state, and time-resolved fluorescence emission of solutions of OG488 at pH 4.60 and total acetate/acetic acid concentration between 0.1 and 1 M. The absorption spectra of these solutions were essentially equal. Only slight differences, due to ionic strength effects, were noticed. The steady-state fluorescence emission spectra showed an increase in intensity with increasing buffer concentration, along with a transformation of the spectral shape from monoanion to dianion shape, as explained previously.[5] The time-resolved fluorescence decay traces of these solutions were recorded using the experimental setups mentioned in Materials and Methods. The decay traces at the same total acetate buffer concentration were globally analyzed, with the decay times linked as shared parameters, whereas the pre-exponential factors were local adjustable parameters. All the decay traces were well fitted by

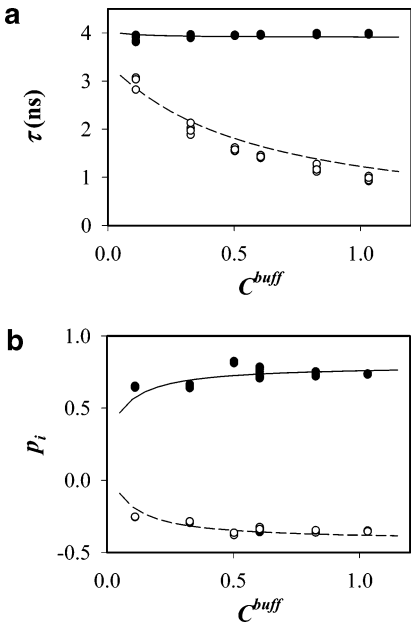

Figure 4. (a) Decay times (● and ○) recovered by global analyses of decay traces from OG488 aqueous solutions at pH 4.60 and increasing acetate buffer concentration. Lines were calculated using eq 4 and the following rate constant values: $k_{0D} = 2.47 \times 10^8$ s^{-1}, $k_{0M} = 2.94 \times 10^8$ s^{-1}, $k_{MD} \times [H^+] = 0$, $k_{DM} = 3.57 \times 10^6$ s^{-1}, $k_{MD}^b = 1.79 \times 10^8$ M^{-1} s^{-1}, $k_{DM}^b = 9.70 \times 10^8$ M^{-1} s^{-1}. (b) Corrected pre-exponential factors (● and ○), at $\lambda^{ex} = 420$ nm and $\lambda^{em} = 515$ nm, associated with the decay times of panel a. Lines were calculated by means of eqs 15, using the rate constant values mentioned above, $K_a = 10^{-4.69}$, $\epsilon_R = 0.283$, $c_R = 0.210$, and an arbitrary factor κ' to normalize the lines to the experimental results.

biexponential functions, showing a rise-time (negative associated pre-exponential) as expected due to the deprotonation of the excited monoanion to dianionic form. Figure 4a shows the recovered decay times as symbols, whereas symbols in Figure 4b are the associated pre-exponential factors (corrected as detailed in Materials and Methods) at $\lambda^{ex} = 420$ nm and $\lambda^{em} = 515$ nm.

The decay times can be predicted by means of eq 4, as long as the rate constant values k_{ij} are known. To check the validity of the rate constant values provided in our previous paper, we have calculated the decay times as a function of the total buffer concentration, at pH = 4.60. Figure 4a shows the good agreement between the calculated decay times (lines) and those recovered from global analyses of the decay traces. We have also calculated the pre-exponential values vs total buffer concentration at the same pH value. Figure 4b shows good agreement between the corrected pre-exponential factors at $\lambda^{ex} = 420$ nm and $\lambda^{em} = 515$ nm and those calculated using eqs 15. The lines in Figure 4a,b were calculated using the parameters recovered by neglecting the ionic strength effects from our previous paper, in which we demonstrated the low influence of these effects:[5] The use of the parameters and equations taking into account the ionic strength resulted in essentially the same curves, but a much more complicated model.

From the values of the kinetic and spectral parameters which we have obtained through analysis of the fluorescence decay traces, we can also predict the steady-state fluorescence intensities at constant pH and different buffer concentrations, by means of the integral in eq 13. We have simulated the steady-state fluorescence intensity as a function of the total buffer concentration, at three different constant pH values (4.00, 4.30, and 4.60), with $\lambda^{ex} = 420$ nm and $\lambda^{em} = 515$ nm. Symbols in Figure 5 represent the experimental steady-state fluorescence emission

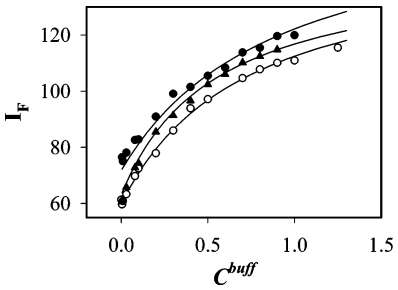

Figure 5. Increase in steady-state fluorescence intensity ($\lambda^{ex} = 420$ nm, $\lambda^{em} = 515$ nm) with increasing buffer concentration, at pH values 4.00 (●), 4.30 (○), and 4.60 (▲). Lines were calculated using eqs 4, 13, and 15 with $k_{0D} = 2.47 \times 10^8$ s^{-1}, $k_{0M} = 2.94 \times 10^8$ s^{-1}, $k_{MD} \times [H^+] = 0$, $k_{DM} = 3.57 \times 10^6$ s^{-1}, $k^b_{MD} = 1.79 \times 10^8$ M^{-1} s^{-1}, $k^b_{DM} = 9.70 \times 10^8$ M^{-1} s^{-1}, $K_a = 10^{-4.69}$, $\epsilon_R = 0.283$, and $c_R = 0.210$ and normalized with the corresponding experimental value at $C^{buff} = 0.9$ M.

(here we included the series I_F vs C^{buff}, published before,[5] at the pH values mentioned above, $\lambda^{ex} = 420$ nm, and $\lambda^{em} = 515$ nm), whereas the lines are the simulated steady-state fluorescence intensities. The agreement between both fluorescence signals is excellent. Hence, our recovered pertinent parameters permit evaluation of the steady-state fluorescence signal and decay times at any pH and C^{buff}.

Conclusions

Since the presence of excited-state buffer-mediated proton exchange reactions may result in distorted steady-state fluorescence signals, we have examined how the specific rate constants, along with the time-resolved emission data, correlate with steady-state fluorescence spectra. We have demonstrated that kinetic and spectral parameters from time-resolved emission data, and global analysis and global compartmental analysis, can be used to calculate the characteristic decay times for different conditions of dye solutions (any pH and any buffer concentration) and steady-state fluorescence intensity (any pH and any buffer concentration). The good agreement between the theoretical calculations and the experimental data demonstrates that global compartmental analysis is a powerful tool to recover kinetic parameters from complex and challenging systems, such as aqueous solutions of OG488. The correlation of the time-resolved fluorescence parameters with the steady-state fluorescence emission intensity requires the evaluation of the ratio of either the associated pre-exponentials or the individual corrected pre-exponential factors from fluorescence decay traces whose relative amplitudes have been adjusted so that they are equivalent to those recorded for the same time interval and the same optical setup. In this work, we obtained better results through the second methodology.

Acknowledgment. A.O. thanks the Spanish Ministry of Education and Science for a predoctoral fellowship. This work was supported by Grant BQU2002-01311 from the Spanish Ministry of Science and Technology.

References and Notes

(1) Haugland, R. P. *Handbook of Fluorescent Probes and Research Products*, 9th ed.; Molecular Probes, Inc.: Eugene, OR, 2002.

(2) (a) Vergne, I.; Constant, P.; Lanéelle, G. *Anal. Biochem.* **1998**, *255*, 127−132. (b) Gee, K. R. *Bioorg. Med. Chem. Lett.* **1999**, *9*, 1395−1396. (c) Thomas, D.; Tovey, S. C.; Collins, T. J.; Bootman, M. D.; Berridge, M. J.; Li, P. *Cell Calcium* **2000**, *28*, 213−223. (d) Goodnough, M. C.; Oyler, G.; Fishman, P. S.; Johnson, E. A.; Neale, E. A.; Keller, J. E.; Te, W. H.; Clark, M.; Hartz, S.; Adler, M. *FEBS Lett.* **2002**, *513*, 163−168. (e) Rusinova, E.; Tretyachenko-Ladokhina, V.; Vele, O. E.; Senear, D. F.; Alexander Ross, J. B. *Anal. Biochem.* **2002**, *308*, 18−25.

(3) Alvarez-Pez, J. M.; Ballesteros, L.; Talavera, E.; Yguerabide, J. *J. Phys. Chem. A* **2001**, *105*, 6320−6332.

(4) Crovetto, L.; Orte, A.; Talavera, E. M.; Alvarez-Pez, J. M.; Cotlet, M.; Thielemans, J.; De Schryver, F. C.; Boens, N. *J. Phys. Chem. B* **2004**, *108*, 6082−6092.

(5) Orte, A.; Crovetto, L.; Talavera, E. M.; Boens, N.; Alvarez-Pez, J. M. *J. Phys. Chem. A* **2005**, *109*, 734−747.

(6) (a) Beechem, J. M.; Ameloot, M.; Brand, L. *Chem. Phys. Lett.* **1985**, *120*, 466−472. (b) Ameloot, M.; Beechem, J. M.; Brand, L. *Chem. Phys. Lett.* **1986**, *129*, 211−219. (c) Van den Bergh, V.; Boens, N.; De Schryver, F. C.; Ameloot, M.; Gallay, J.; Kowalczyk, A. *Chem. Phys.* **1992**, *166*, 249−258.

(7) Boens, N.; Basarić, N.; Novikov, E.; Crovetto, L.; Orte, A.; Talavera, E. M.; Alvarez-Pez, J. M. *J. Phys. Chem. A* **2004**, *108*, 8180−8189.

(8) Lakowicz, J. R. *Principles of Fluorescence Spectroscopy*; Kluwer Academic/Plenum Publishers: New York, 1999.

(9) Ameloot, M.; Boens, N.; Andriessen, R.; Van den Bergh, V.; De Schryver, F. C. *J. Phys. Chem.* **1991**, *95*, 2041−2047.

(10) Diehl, H.; Horchak-Morris, N. *Talanta* **1987**, *34*, 739−741.

(11) Johnson, M. L.; Frasier, S. G. *Methods Enzymol.* **1985**, *117*, 301−342.